



Microarcsecond optical astronomy

Dr. Eugen Pavel

Storex Technologies, Bucharest, Romania

IAA Seminar – May 13, 2026, Bucharest, Romania

Summary

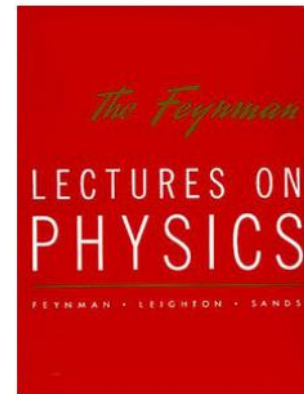
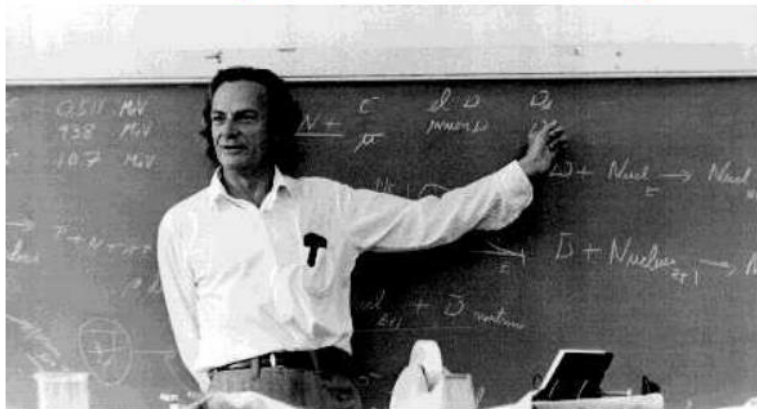
- **Introduction**
- **Modified Thomas Young's double-slit experiment**
- **Insensitivity of QCE detectors to seeing conditions**
- **Measurements of double-line spectroscopic binary systems:**
 - i) Capella (α Auriga)**
 - ii) Spica (α Vir)**
- **Conclusions**

Introduction (1)

- **Christiaan Huygens (1690)**
- **Isaac Newton (1704)**
- **Thomas Young (1803); August Fresnel (1815)**
- **Albert Einstein (1905); Arthur H. Compton (1923)**

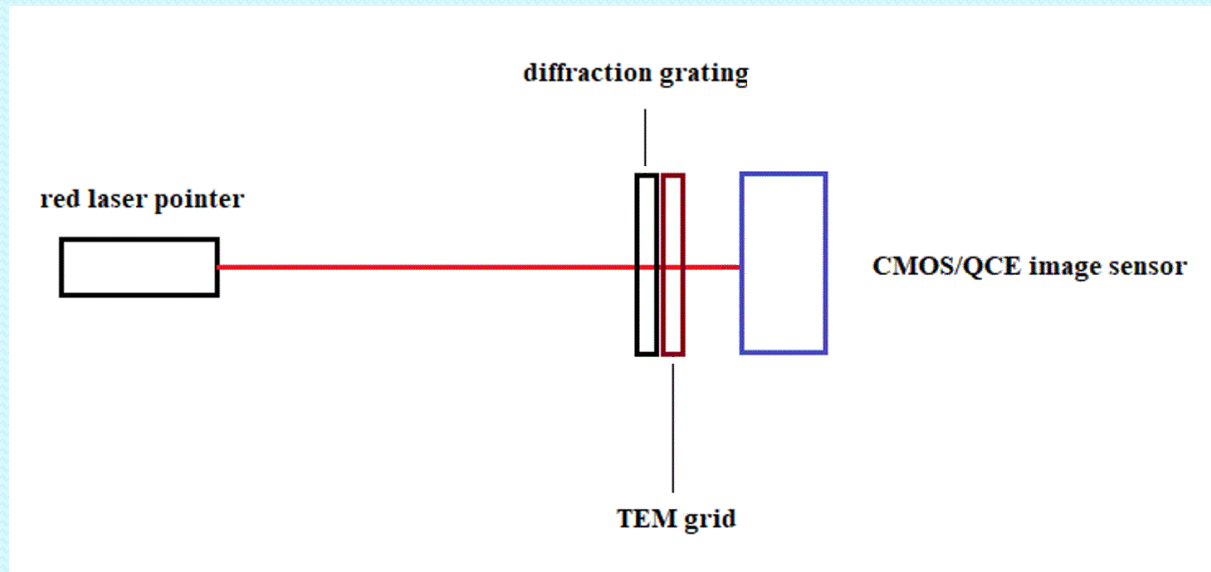
Introduction (2)

Wave particle duality: one of the “great mysteries” of quantum mechanics



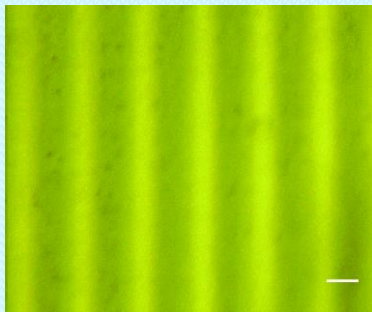
In this chapter we shall tackle immediately the basic element of the mysterious behavior in its most strange form. We choose to examine a phenomenon which is impossible, *absolutely* impossible, to explain in any classical way, and which has in it the heart of quantum mechanics. In reality it contains the only mystery*. Vol. 3, chapter 18

Modified Thomas Young's double-slit experiment (1)

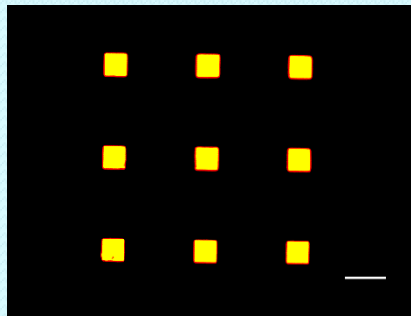


Experimental system used in multiple slit measurements.

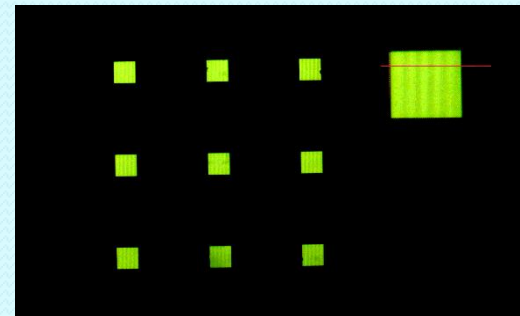
Modified Thomas Young's double-slit experiment (2)



a)



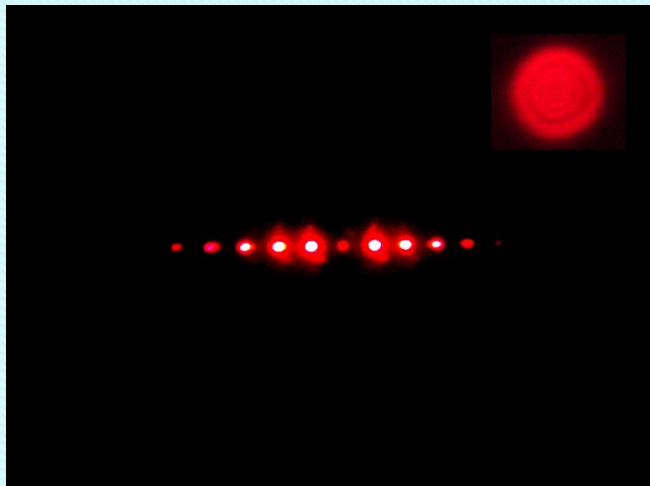
b)



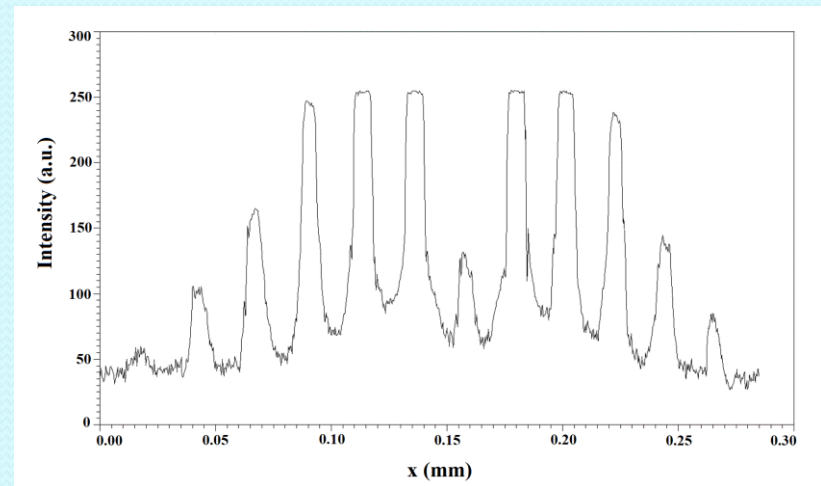
c)

Optical microscope images of: a) 50L grating, scale bar: 10 μm ; b) TEM grid, scale bar: 200 μm ; c) ensemble of 50L grating and TEM grid; insert: detailed image of a window.

Modified Thomas Young's double-slit experiment (3)



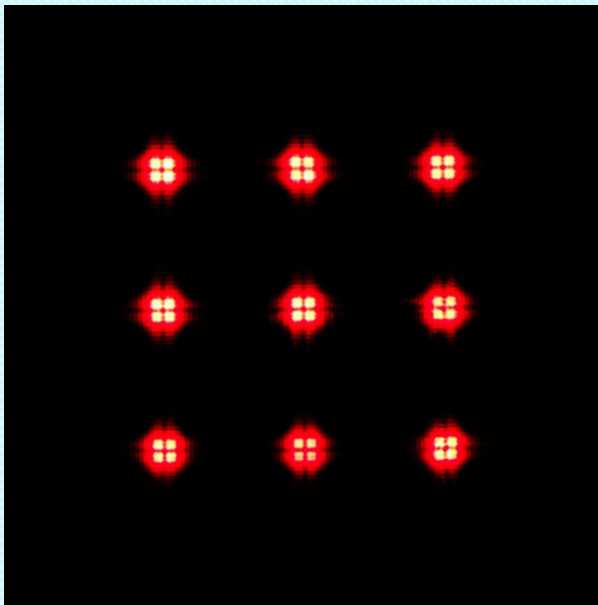
a)



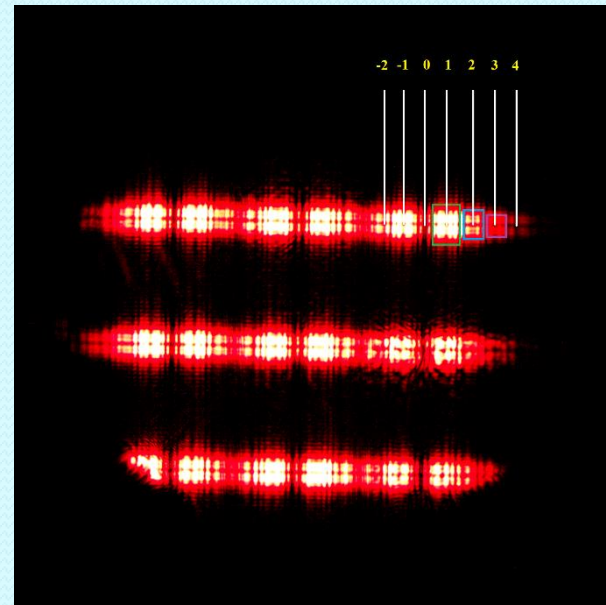
b)

a) Diffraction pattern of the laser pointer recorded in transmittance mode from 50L grating. The distance from the grating to the screen was $D_1 = 250$ mm. Insert: CMOS sensor image of TEM (4,0) cylindrical transversal mode of the laser beam; b) diffraction efficiency of grating (0, 1, 2, 3, 4, 5 orders).

Modified Thomas Young's double-slit experiment (4)



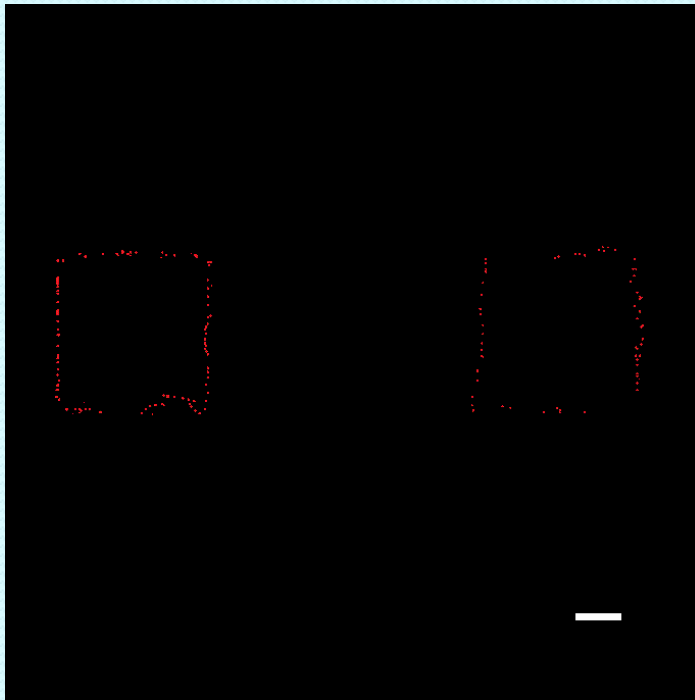
a)



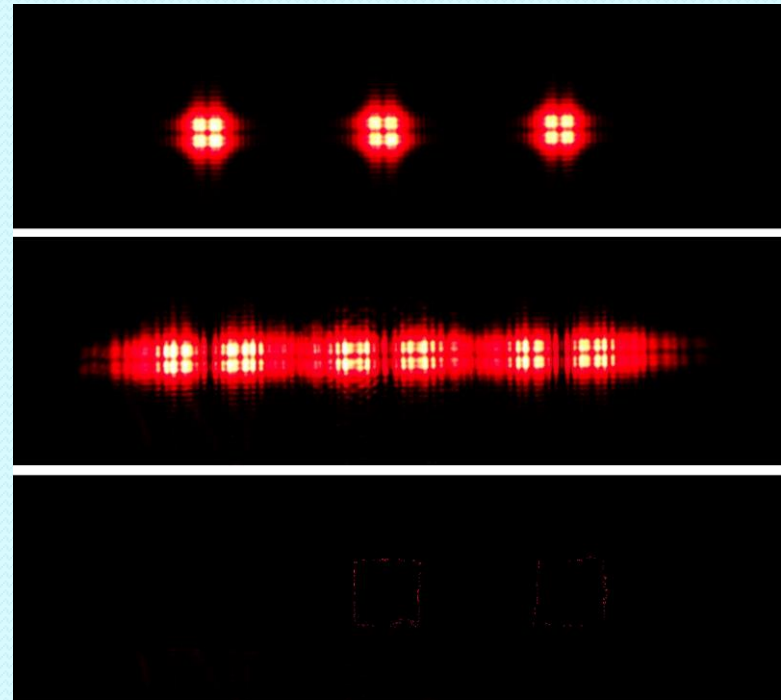
b)

a) CMOS image of the rectangular transverse mode TEM (1,1) recorded in transmittance mode from TEM grid; b) CMOS image of the diffraction patterns recorded in transmittance mode from 50L grating and TEM grid ensemble.

Modified Thomas Young's double-slit experiment (5)



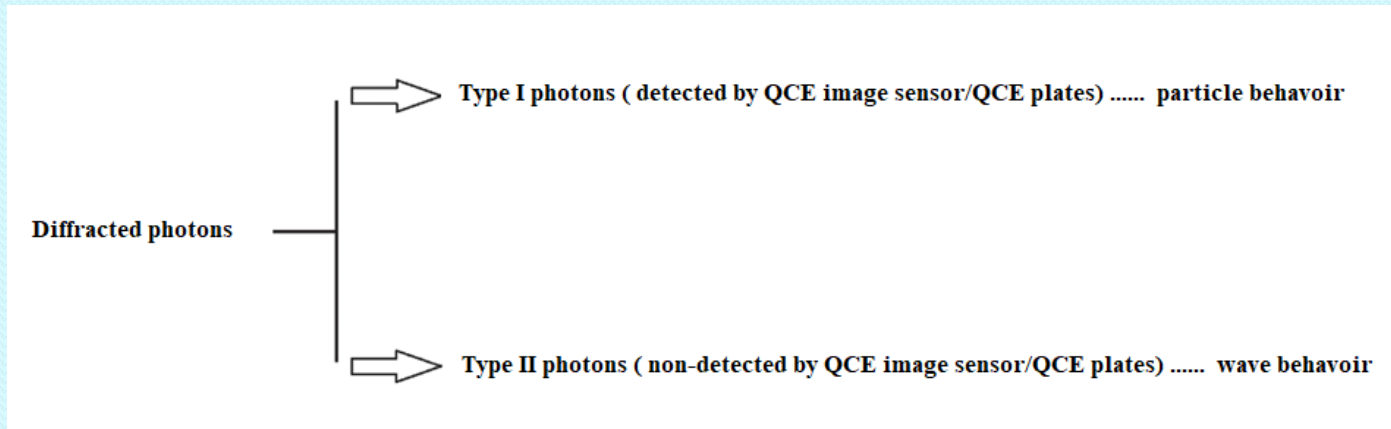
a)



b)

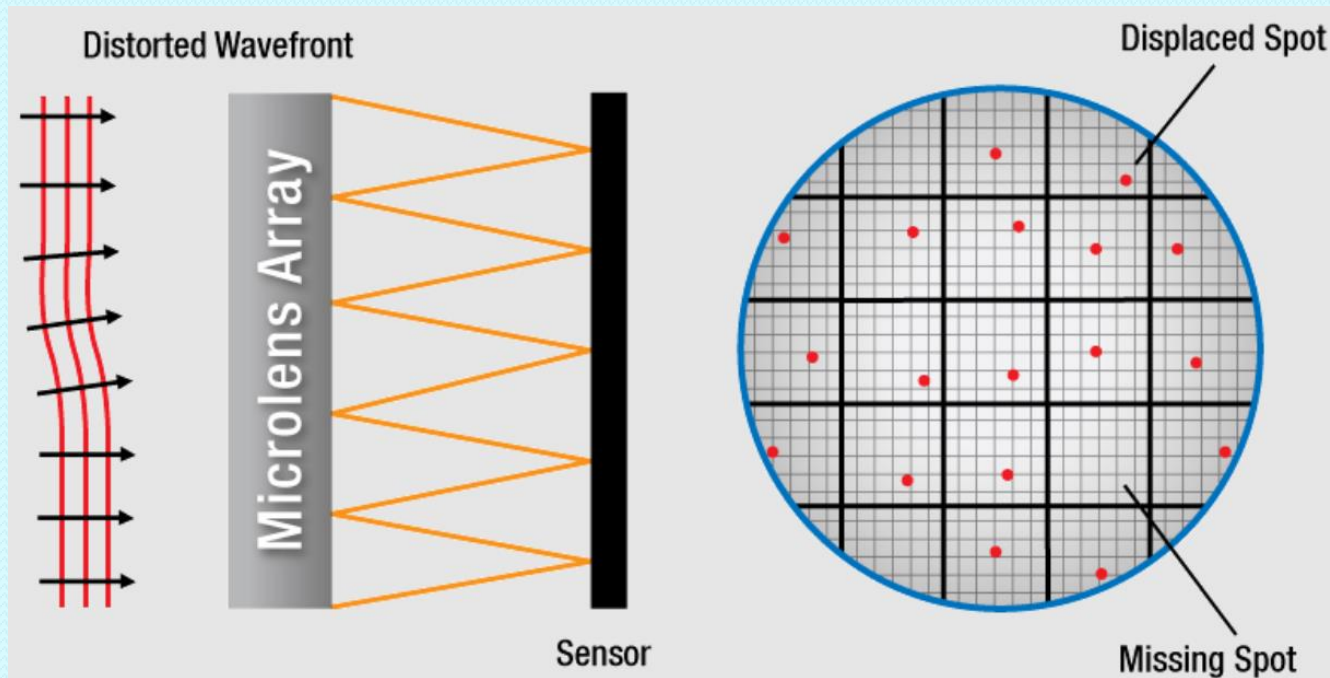
a) QCE image of the pattern recorded in transmittance mode from 50L grating and TEM grid sandwich; b) rows of CMOS images of 3 windows of TEM grid without (upper row) and with diffraction grating (middle row) and QCE image with diffraction grating (lower row).

Modified Thomas Young's double-slit experiment (6)



Classification of the diffracted photons.

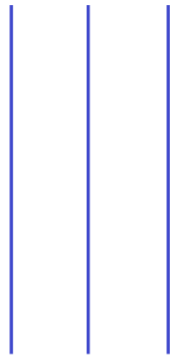
Insensitivity of QCE detectors to seeing conditions (1)



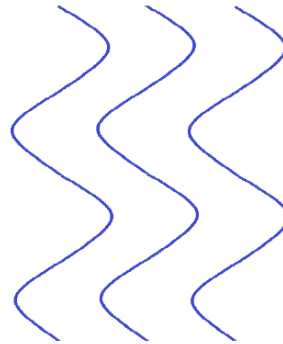
Shack Hartmann wavefront sensor.

Inensitivity of QCE detectors to seeing conditions (2)

Plane wavefront inside QCE layer



Distorted wavefront



**Shack Hartmann
wavefront sensor**

Wavefronts inside QCE layer and before Shack Hartmann wavefront sensor.

Measurements of double-line spectroscopic binary systems (1)

Estimated separation resolution of QCE plates used for microarcsecond optical astronomy.

Telescope	Gran Telescopico Canarias	Very Large Telescope (VLT)	Hubble Space Telescope	J. Webb Space Telescope	Hooker Telescope	N150/750 with a 30x stacked Barlow lenses
Diameter (m)	10.4	4 x 8.2	2.4	6.5	2.54	0.15
Focal length (m)	169.9	120	57.6	131.4	12.7	22.5
Ratio (F/F _{ref})	113	80	38	87	8.4	30
Separation sensitivity* (nm/mas)	~226**	~160**	~76**	~175**	~16.9**	~170
Estimated separation resolution*** (μas/nm)	~4	~6	~13	~6	~59	~6

*Separation sensitivity = (Reference separation sensitivity) *Ratio(F/F_{ref});

**Reference separation sensitivity is selected 2 nm/mas [31].

***Estimated separation resolution = 1/ (Separation sensitivity)

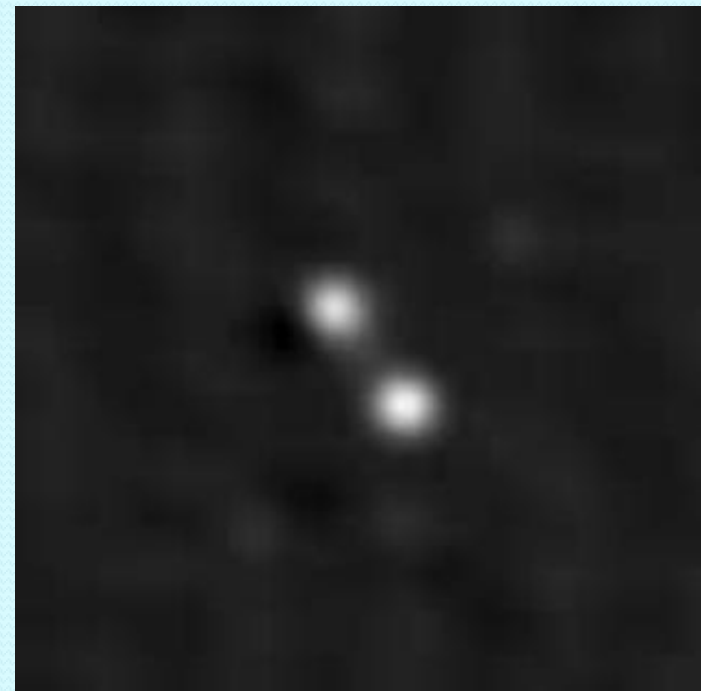
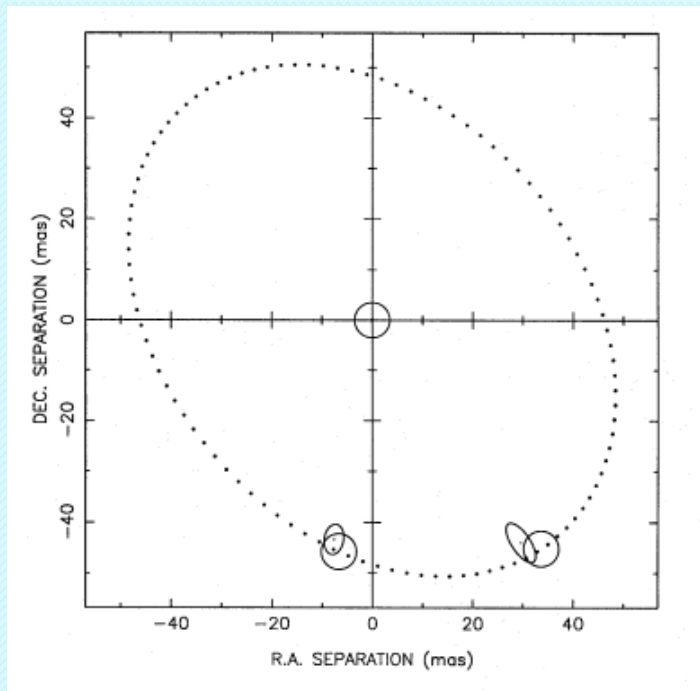


Measurements of double-line spectroscopic binary systems (2)

Comparison of equipment used in astronomical imaging.

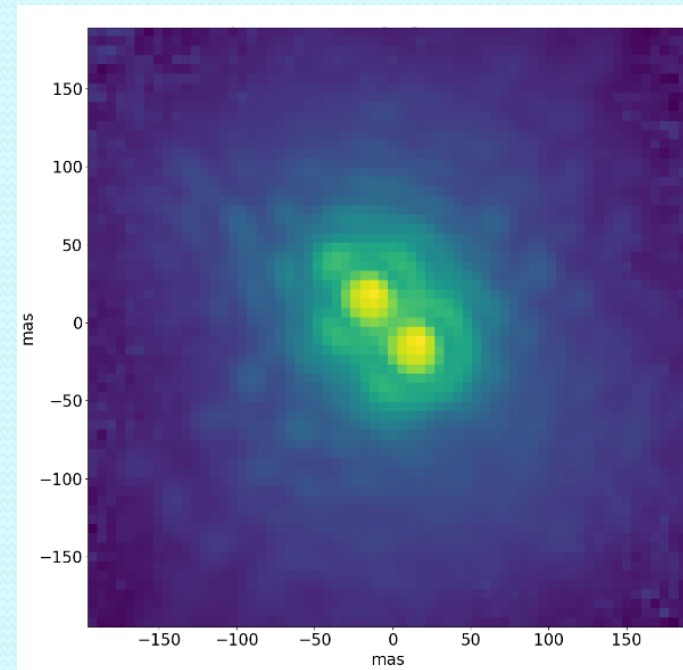
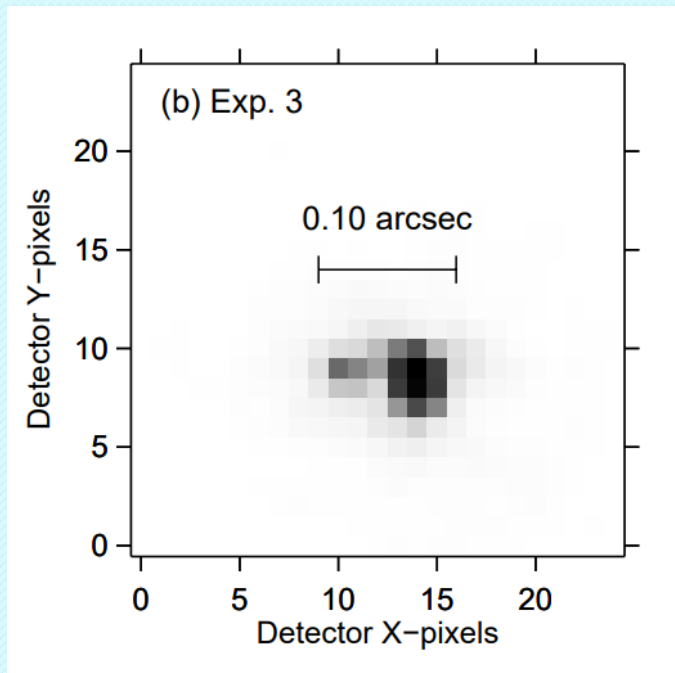
Equipment	Main characteristics		Cost	Operational complexity	Applicable celestial types
	Diffraction	Seeing conditions			
Adaptive optics telescopes	limited	sensitive	very high	high	all types
Optical interferometers	limited	sensitive	high	very high	bright stars
QCE image sensor/QCE plates mounted on telescopes	diffractionless	insensitive	low	low	R&D

Measurements of double-line spectroscopic binary systems - Capella (3)



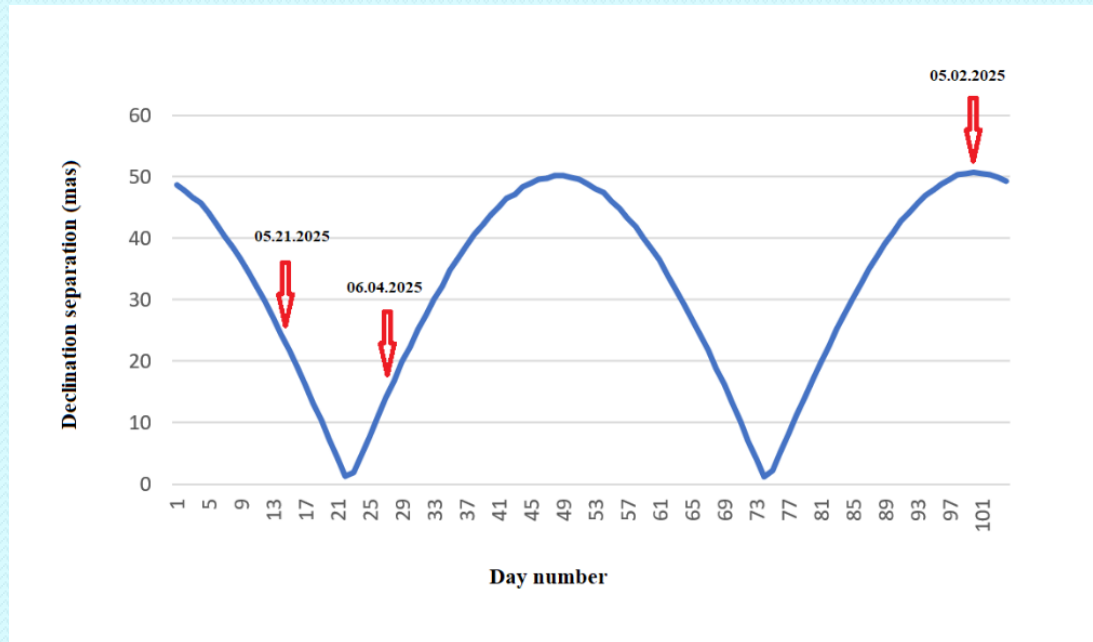
- a) The apparent orbit of Capella. *Astronomy and Astrophysics*, **306**, L13–L16 (1996).
- b) Reconstruction image from optical interferometric data of Capella on September 13, 1995 (Mullard Radio Astronomy Observatory, Cambridge).

Measurements of double-line spectroscopic binary systems - Capella (4)



- a) Hubble Space Telescope image of Capella on December 21, 1997 with 250-300 nm filter.
The Astrophysical Journal **565** (2002) 598-607
- b) Visible-light imaging of the Capella double star with SCEAO/VAMPIRES dual-band imager, of Subaru Telescope.

Measurements of double-line spectroscopic binary systems - Capella (5)



Declination separation of Capella (α Auriga) stars Aa, Ab as a function of the day number in the orbital period. The red arrows indicate the observation dates.

E. Pavel, V. Marinescu, "Spatially resolving spectroscopic binaries by diffractionless telescope with Type I diffracted photons", *Optik* **348** (2026) 172709.

Measurements of double-line spectroscopic binary systems - Capella (6)

Table 1. Measurements of Capella (α Auriga) with QCE plates

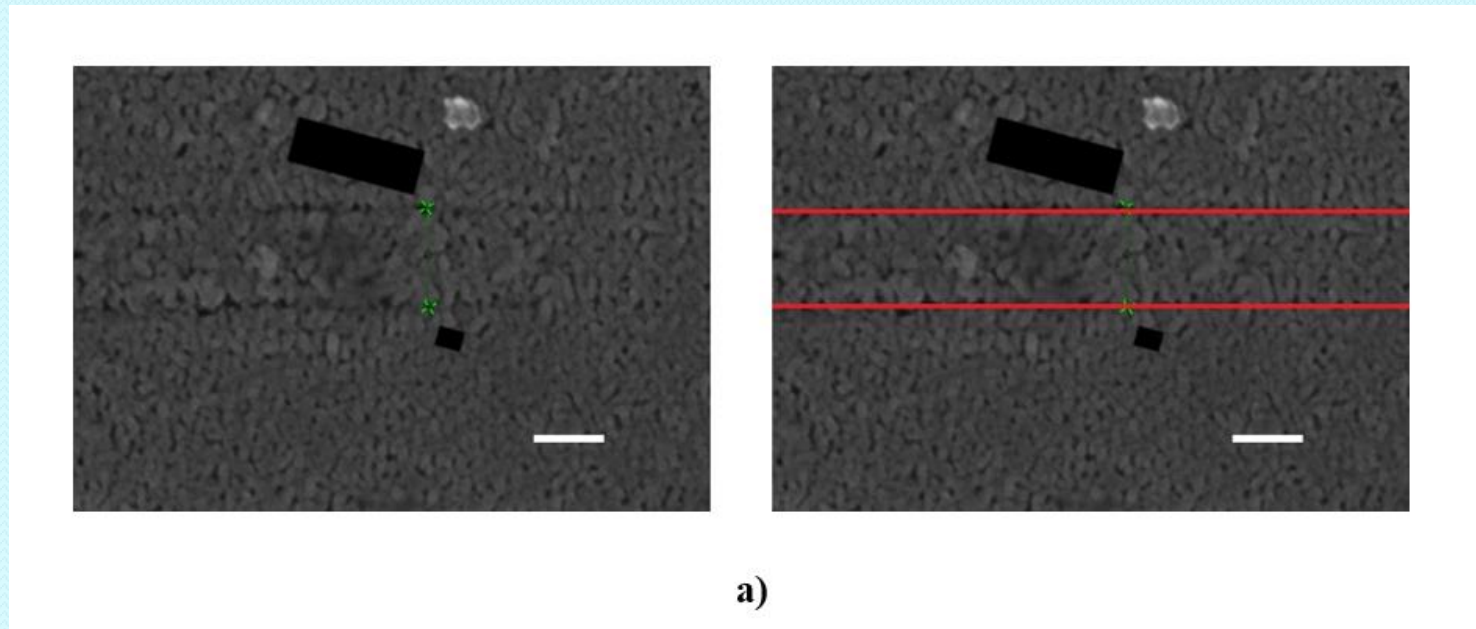
Observation date (UT)	Observation date (JD)	Day number in the orbital period	Declination separation	Geometric line separation* (nm)	Measured line separation (nm)	Separation sensitivity (nm/mas)	QCE reduction** (x)	Seeing conditions [48] (arcsecond)
2025 May 2	2,460,798.33	99	50.50	367	~128	~2.53	~2.86	1.41
2025 May 21	2,460,817.33	14	24.33	176	~70	~2.87	~2.51	1.36
2025 June 4	2,460,831.33	28	16.77	121	~58	~3.45	~2.08	1.20

*Geometric line separation: $d = F \times \tan(\alpha)$; F = focal length; α = declination separation

**QCE reduction = (Geometric line separation)/(Measured line separation)

E. Pavel, V. Marinescu,” Spatially resolving spectroscopic binaries by diffractionless telescope with Type I diffracted photons”, *Optik* **348** (2026) 172709.

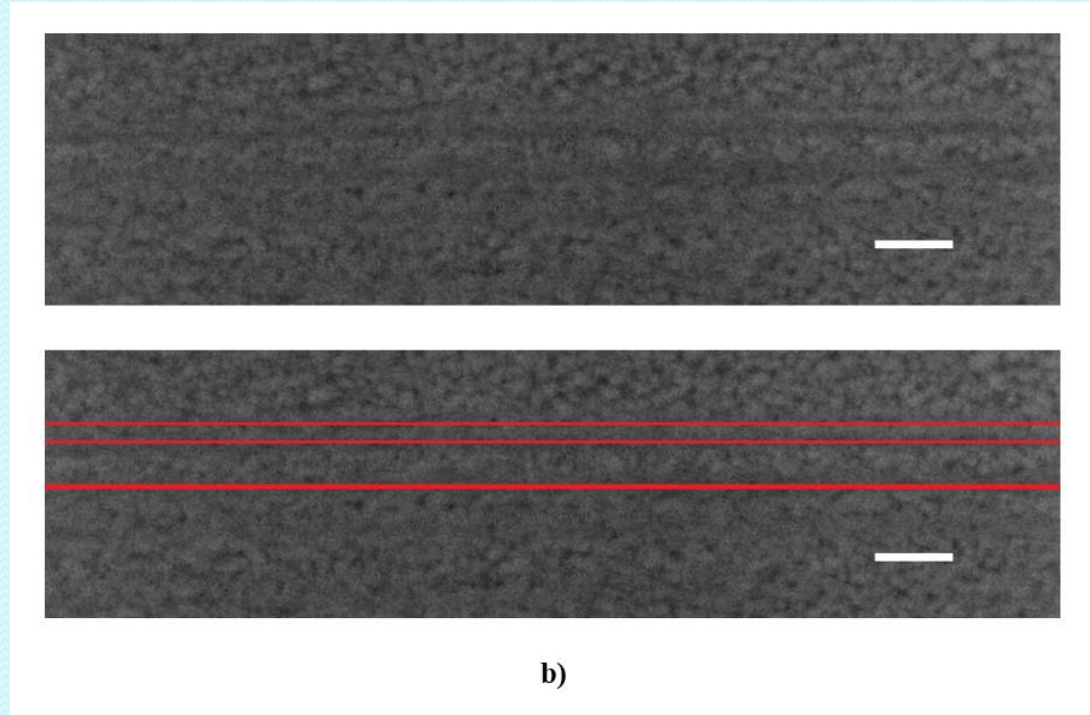
Measurements of double-line spectroscopic binary systems - Capella (7)



The passage images of Capella (α Auriga), captured by a N150/750 telescope with 2x Barlow lens on: a) May 2, 2025.

E. Pavel, V. Marinescu, "Spatially resolving spectroscopic binaries by diffractionless telescope with Type I diffracted photons", *Optik* **348** (2026) 172709.

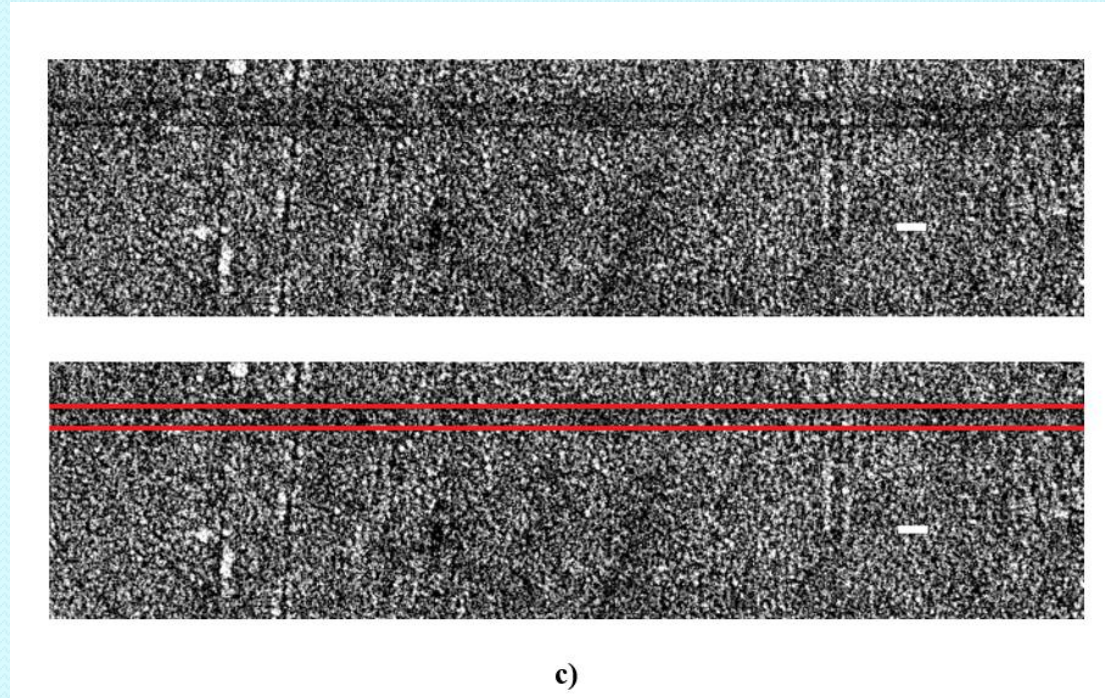
Measurements of double-line spectroscopic binary systems - Capella (8)



The passage images of Capella (α Auriga), captured by a N150/750 telescope with 2x Barlow lens on: b) May 21, 2025.

E. Pavel, V. Marinescu,” Spatially resolving spectroscopic binaries by diffractionless telescope with Type I diffracted photons”, *Optik* **348** (2026) 172709.

Measurements of double-line spectroscopic binary systems - Capella (9)



The passage images of Capella (α Auriga), captured by a N150/750 telescope with 2x Barlow lens on: c) May 2, 2025.

E. Pavel, V. Marinescu, "Spatially resolving spectroscopic binaries by diffractionless telescope with Type I diffracted photons", *Optik* **348** (2026) 172709.

Measurements of double-line spectroscopic binary systems - Capella (10)

Measurements of Capella Aa (α Auriga) with QCE plates

Object	Observation date (UT)	Observation date (JD)	Angular diameter (mas)	Geometric image of angular diameter* (nm)	Measured image of angular diameter (nm)	Separation sensitivity (nm/mas)	QCE reduction (x)	Seeing conditions [31] (arcsecond)
Capella Aa (α Auriga)	2025 May 21	2,460,817.04	8.46 [49]	61	~24	~2.83	~2.54	1.36

*Geometric image of angular diameter: $d = F \times \tan(\alpha)$; F = focal length; α = angular diameter

E. Pavel, V. Marinescu,” Spatially resolving spectroscopic binaries by diffractionless telescope with Type I diffracted photons”, *Optik* **348** (2026) 172709.

Measurements of double-line spectroscopic binary systems - Spica (11)



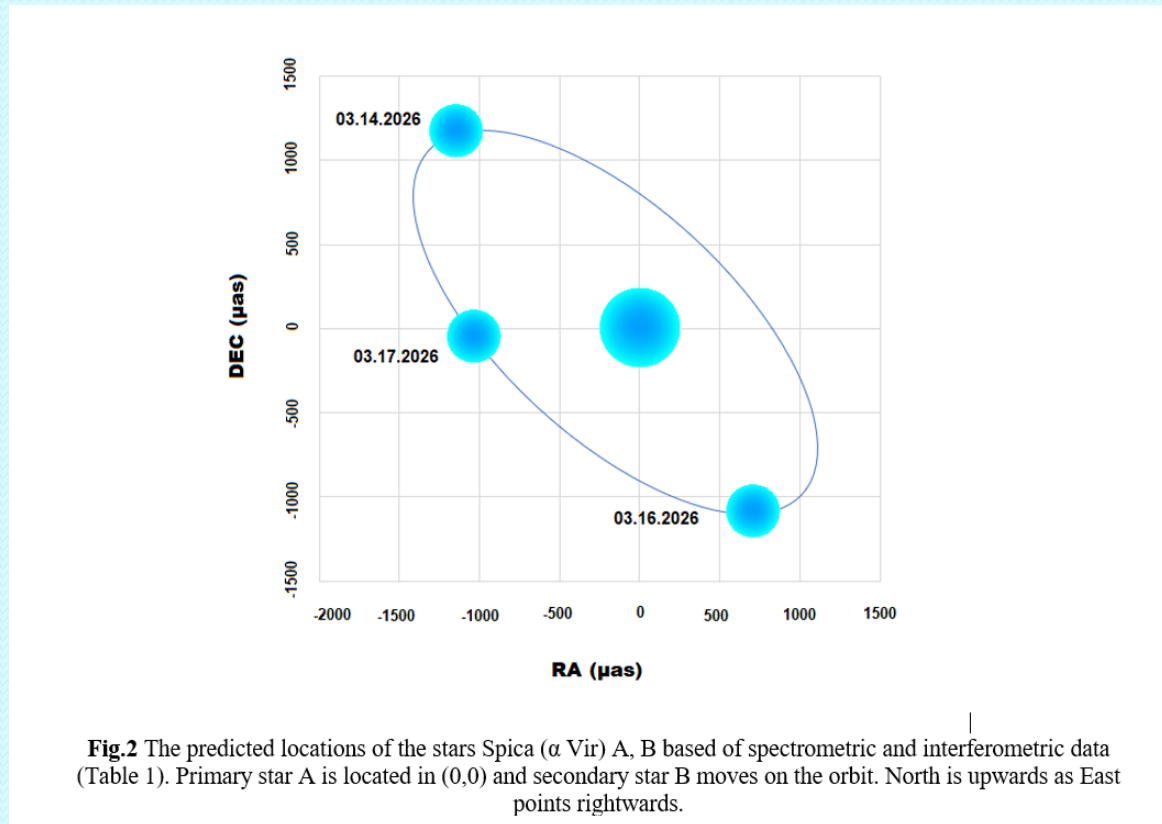
CCD camera image of a neon sign located 1700 m away from an N150/750 telescope with a 30x stacked Barlow lenses. The inset at the top right is an image captured by the CCD camera of the same neon sign, taken with the N150/750 telescope without a Barlow lens.

Measurements of double-line spectroscopic binary systems - Spica (12)

Table 1 Spica model parameters (orbital elements).

Parameter name	Value	Reference
Orbital period (P)	4.0145898 days	[14]
Epoch of periastron (T)	JD: 2440678.09	[14]
Eccentricity (e)	0.133	[2]
Semimajor axis (a)	1.54 mas	[14]
Inclination (i)	63.1°	[2]
Position angle of the ascending node (Ω)	130.4°	[3]
Argument of periastron (ω)	312°	Present study
Period of rotation of line of apsides (U)	124 y	[14]

Measurements of double-line spectroscopic binary systems - Spica (13)



Measurements of double-line spectroscopic binary systems - Spica (14)

Predicted values of Spica parameters.

Observation date	JD	Orbital phase	ν (true anomaly) ($^{\circ}$)	DEC (μas)	RA (μas)	θ ($^{\circ}$)	ρ (μas)
March 14, 2026	2461113.500000	0.710	241	1170	-1078	317	1578
March 16, 2026	2461115.416667	0.187	82	-1098	676	148	1283
March 17, 2026	2461116.416667	0.436	162	-58	-1028	266	1010

Measurements of double-line spectroscopic binary systems - Spica (15)

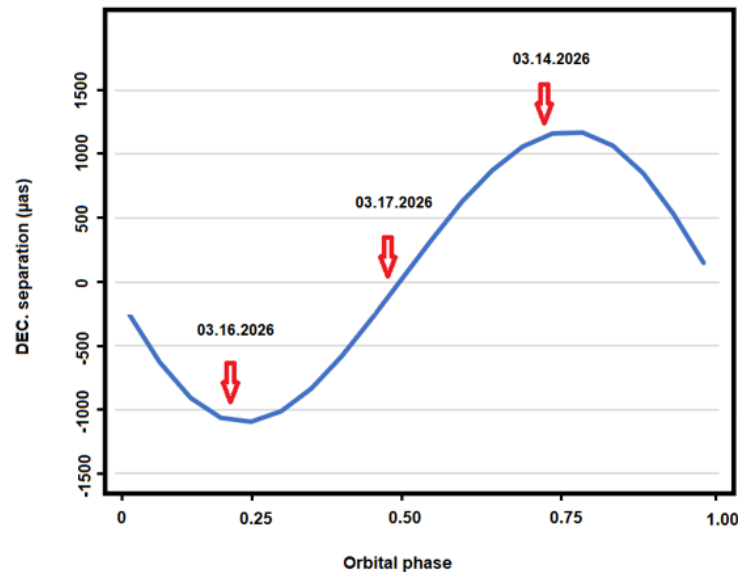


Fig.3 The declination separation of the stars Spica (α Vir) A and B as a function of orbital phase. The red arrows indicate the observation dates in MM/DD/YYYY format.

Measurements of double-line spectroscopic binary systems - Spica (16)

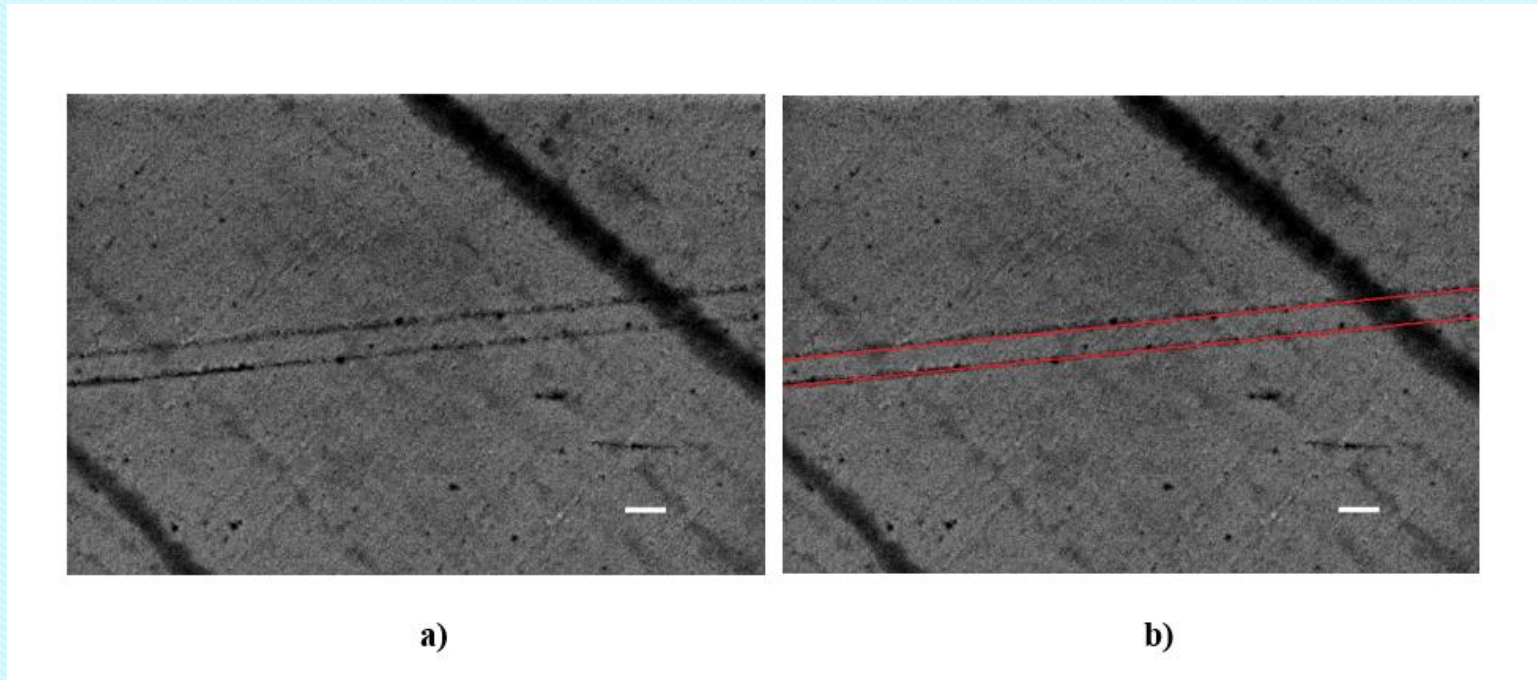
Measurements of Spica (α Vir) with QCE plates.

Observation date (UT)	Observation date (JD)	Day number in the orbital period	Declination separation (mas)	Geometric line separation* (nm)	Measured line separation (nm)	Separation sensitivity (nm/mas)	Estimated separation resolution (μ as/nm)	QCE factor** (x)	Seeing conditions [39] (arcsecond)
March 14, 2026	2461113.500000	3	1.170	127	~210	~179	~6	~0.6	1.48
March 16, 2026	2461115.416667	1	-1.098	119	~190	~171	~6	~0.6	1.86
March 17, 2026	2461116.416667	2	-0.058	6	~160	~2758	~0.4	~0.04	2.17

*Geometric line separation: $d = F \times \tan(\alpha)$; F = focal length; α = declination separation

**QCE factor = (Geometric line separation)/(Measured line separation)

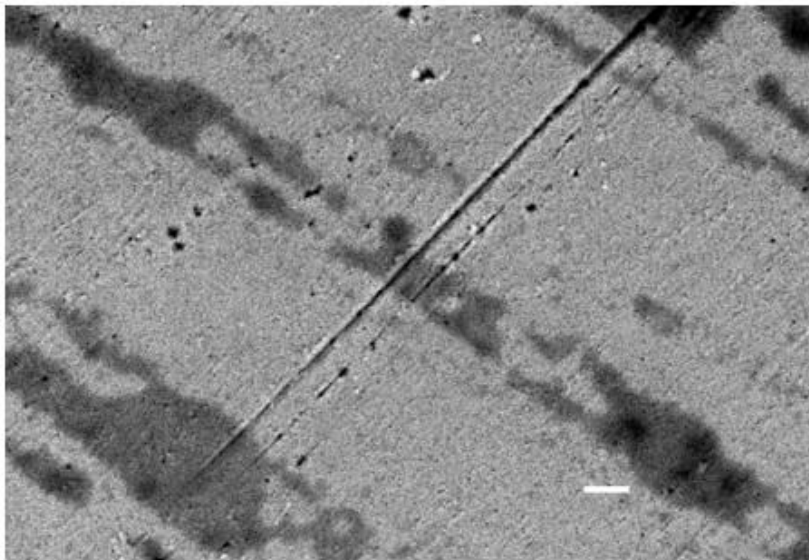
Measurements of double-line spectroscopic binary systems - Spica (17)



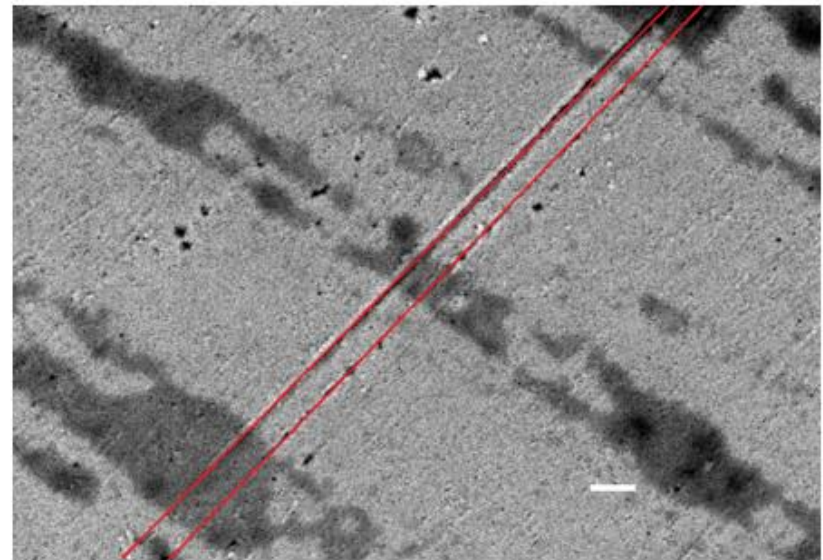
The passage images of Spica (α Vir) captured by a N150/750 telescope with a 30x stacked Barlow lenses on: a, b) March 14, 2026; scale bars 300 nm; (red lines are guides for eye and represents the recorded lines of star tracking).

E. Pavel, V. Marinescu, "Microarcsecond optical astronomy with Type I diffracted photons", *Optica Open ID:131510* (2026).

Measurements of double-line spectroscopic binary systems - Spica (18)



c)

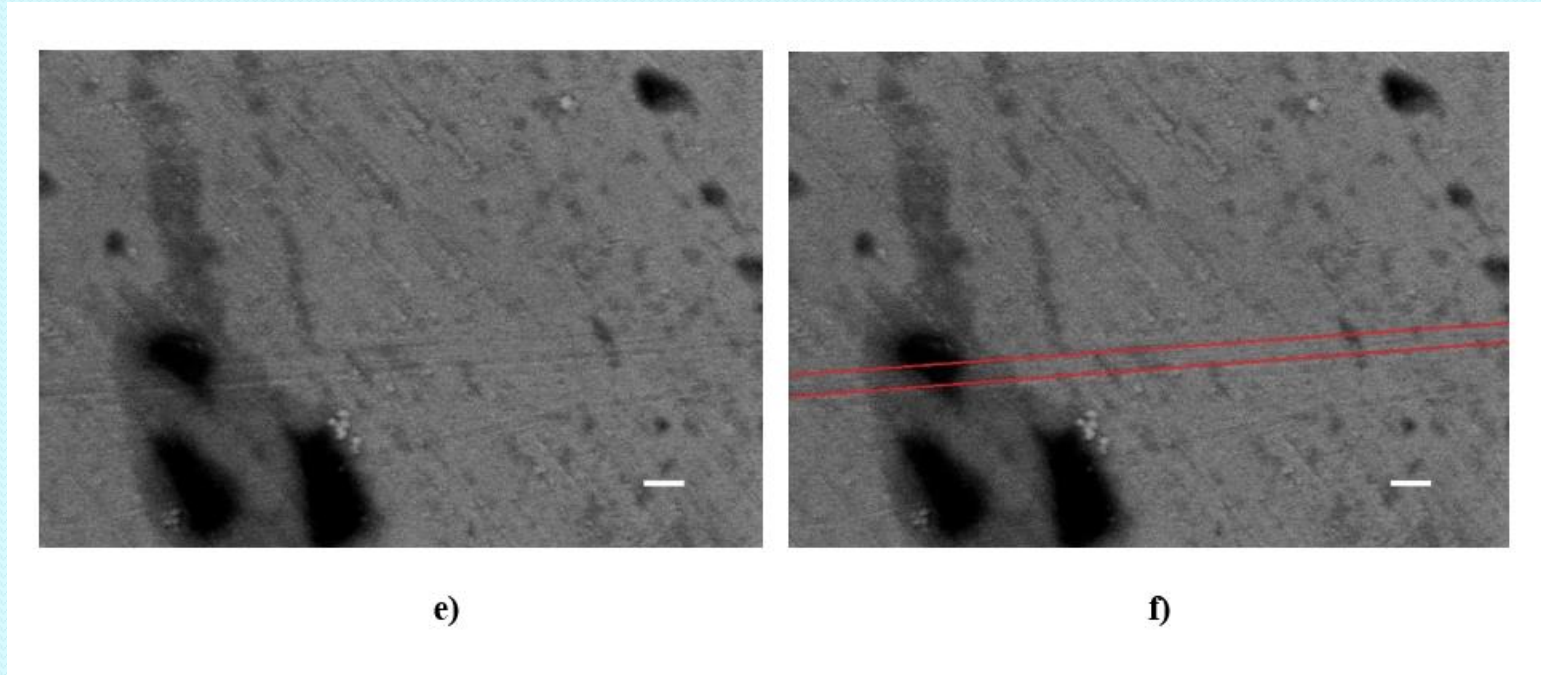


d)

The passage images of Spica (α Vir) captured by a N150/750 telescope with a 30x stacked Barlow lenses on: c, d) March 16, 2026; scale bars 300 nm; (red lines are guides for eye and represents the recorded lines of star tracking).

E. Pavel, V. Marinescu, "Microarcsecond optical astronomy with Type I diffracted photons", *Optica Open ID:131510* (2026).

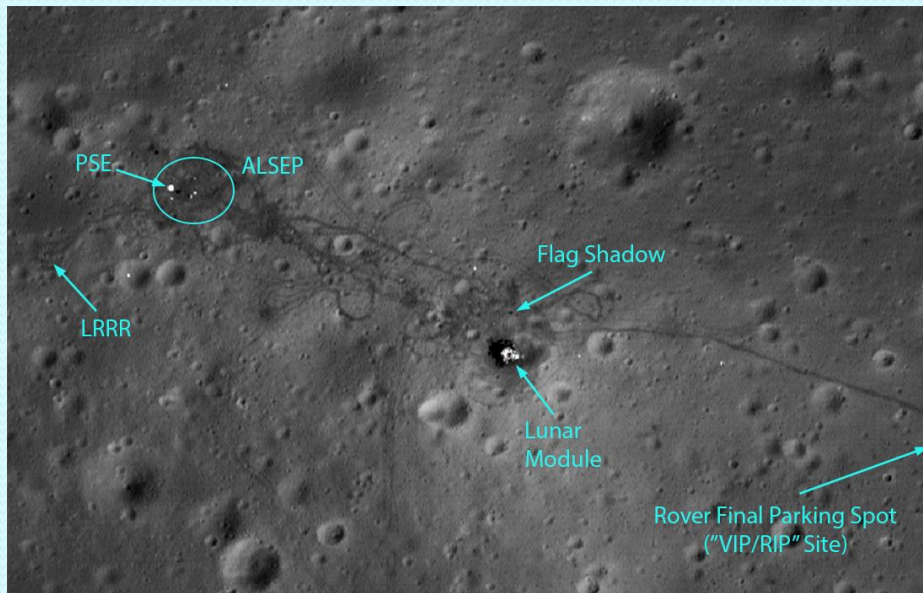
Measurements of double-line spectroscopic binary systems - Spica (19)



The passage images of Spica (α Vir) captured by a N150/750 telescope with a 30x stacked Barlow lenses on: e, f) March 17, 2026; scale bars 300 nm; (red lines are guides for eye and represents the recorded lines of star tracking).

E. Pavel, V. Marinescu, "Microarcsecond optical astronomy with Type I diffracted photons", *Optica Open* ID:131510 (2026).

Conclusions - Moon (1)



Lunar Reconnaissance Orbiter telescope

Cassegrain; $f/3.59$; diameter: 19.5 cm;
Rayleigh diffraction limit $\theta = 0.645$ arcsecond.

Theoretic resolution at 49.9 Km: 0.15 m.
Experimental measurements: 0.27 m/pixel.

Earth-based telescopes

Objects larger than 0.11 m on the Moon's surface can be observed using telescopes with an aperture greater than 15 cm and 30x Barlow lenses, in conjunction with QCE plates (angular resolution $\sim 58 \mu\text{as}$).

The Apollo 15 landing site as seen by the Lunar Reconnaissance Orbiter (NASA).
Image captured from 49.9 Km with a resolution of 27 cm/pixel.

Conclusions - deep space observations (2)



Pillars of Creation images of: a) NASA's Hubble Space Telescope (visible domain) and b) NASA's James Webb Space Telescope (near-infrared domain).

Conclusions (3)

- ❑ A modified Thomas Young's double-slit experiment was realized with Quantum Confinement Effect (QCE) detector. Two types of diffracted photons have been discovered: (i) Type I with particle behavior and (ii) Type II with wave behavior.
- ❑ The separation of the two components Aa and Ab of Capella Aa (α Auriga) was achieved with a small telescope N150/750 with 2x Barlow lens and QCE plates. The angular diameter of Capella Aa (α Auriga) was measured (8 mas).
- ❑ Type I diffracted photons paved the way for the development of microarcsecond optical astronomy. With a small N150/750 telescope equipped with 30x stacked Barlow lenses and QCE plates, it was possible to observe through atmospheric turbulence, beyond the diffraction limit, at an estimated separation resolution of $\sim 6 \mu\text{s/nm}$.
- ❑ Imaging through the atmosphere is improved by QCE detector due Type I diffracted photons with particle behavior. The two components of the star Spica (α Vir), a double-line spectroscopic binary system, were resolved even when the declination separation, was $58 \mu\text{s}$.
- ❑ Microsecond-scale optical astronomy has the potential to be used in various applications, such as: i) exoplanets, ii) planetary and stellar physics, iii) galactic studies (including dark matter, the cosmic distance scale, cosmic expansion, active galactic nuclei (AGN), and supermassive black holes (SMBH)), as well as iv) extragalactic science and cosmology (stellar microlensing, strongly lensed quasars), and finally, a spectacular application, v) live observation, using ground-based telescopes, of human missions on the visible surface of the Moon.

The background is a dark, starry space scene. At the top, there is a glowing blue wave-like shape. The text "Thank you for your attention!" is centered in a bright cyan color.

Thank you for your attention!